Research article

Changxu Liu[a,*], Peng Mao[a,*], Qinghua Guo, Min Han and Shuang Zhang*

Bio-inspired plasmonic leaf for enhanced light-matter interactions

https://doi.org/10.1515/nanoph-2019-0104
Received April 4, 2019; revised May 21, 2019; accepted June 10, 2019

Abstract: The mathematical concept of fractals is widely applied to photonics as planar structures ranging from terahertz resonators, optical antennas, to photodetectors. Here, instead of a direct mathematical abstract, we design a plasmonic leaf with fractal geometry from the outline of a leaf from Wargrave Pink. The enhanced light-matter interactions are observed numerically from the improvement in both absorption and near-field intensification. To demonstrate the effect experimentally, a three-dimensional fractal structure is realised through direct laser writing, which significantly improves the photothermal conversion. By virtue of the self-similarity in geometry, the artificial leaf improves the absorption of a 10-nm-thick gold film with 14× temperature increment compared to flat Au film. Not limited to the proof-of-concept photothermal experiment demonstrated here, the fractal structure with improved light-matter interactions can be utilised in a variety of applications ranging from non-linear harmonic generation, plasmonic-enhanced fluorescence, to hot electron generation for photocatalysis.

Keywords: bio-inspired; fractal; photothermal conversion; plasmonics.

1 Introduction

Fractal is an abstract object that describes the geometry with a high degree of self-similarity [1]. Stimulated by this mathematical concept, different fractal geometries such as Hilbert curves, Sierpinski carpets, and Cayley trees are utilised in a variety of two-dimensional (2D) planar photonic systems, ranging from terahertz resonators [2–5], optical antennas [6, 7] frequency-selective photonic quasi-crystals [8–11], to sub-wavelength focusing [12, 13], photovoltaics [14, 15], surface-enhanced spectroscopy [16, 17], and photodetectors [18]. Meanwhile, fractal-like structures widely exist in nature at different scales, including spiral galaxies, coastlines and lightning bolts, seashells, and parts of living organisms such as the human lungs. With millions of years of optimisation through natural selection, fractal geometries ubiquitously exist in plants from the branch topology to the shape of the leaves.

Natural evolution always stimulates intriguing clues for novel energy-harvesting devices, ranging from passive cooling by Saharan silver ants [19] to broadband solar absorber by black butterfly [20], viola flower [21], or white beetle [22]. Inspired by the leaf of *Geranium x oxonianum* or Wargrave Pink, we apply fractal geometry to form a plasmonic leaf with substantially intensified light-matter interactions. Combing the self-similarity of the fractal geometry and the plasmonic effect of the metallic material, the artificial leaf achieves not only absorption enhancement in a broad spectrum but also near-field enhancement of the light in the same region at different wavelengths. To provide a straightforward illustration of the intensified light-matter interactions, we fabricate the bio-inspired structure through direct laser lithography and implement the photothermal conversion experiment. A prominent temperature increment under one sun is achieved with an ultra-thin (10 nm) Au film, owing to the broadband absorption enhancement from visible to infrared. We attribute such advantages to the 3D fractal geometry of the plasmonic leaf that enlarges the region of interaction between the metallic film and incident light, while previously used planar configurations [2–18] align fractal structures in the plane perpendicular to the direction of light propagation.

[a]**Changxu Liu and Peng Mao:** These authors contributed equally.
***Corresponding authors: Changxu Liu and Shuang Zhang,** School of Physics and Astronomy, University of Birmingham, Birmingham B15 2TT, UK, e-mail: c.liu.4@bham.ac.uk. https://orcid.org/0000-0003-1196-7447 (C. Liu); s.zhang@bham.ac.uk (S. Zhang);
and **Peng Mao,** School of Physics and Astronomy, University of Birmingham, Birmingham B15 2TT, UK; and College of Electronic and Optical Engineering and College of Microelectronics, Nanjing University of Posts and Telecommunications, Nanjing 210023, China, e-mail: p.mao@bham.ac.uk
Qinghua Guo: School of Physics and Astronomy, University of Birmingham, Birmingham B15 2TT, UK
Min Han: National Laboratory of Solid State Microstructures, College of Engineering and Applied Sciences and Collaborative Innovation Centre of Advanced Microstructures, Nanjing University, Nanjing 210093, China

Not limited to the proof-of-concept demonstration utilising the broad absorption, the near-field enhancement of our plasmonic leaf can be applied in many nanophotonic systems such as non-linear optics, hot electron generation, and fluorescence enhancement of quantum dots or dyes.

2 Modelling of the bio-inspired plasmonic leaf

Figure 1A illustrates a picture of Wargrave Pink, a clump-forming evergreen plant found in West Europe. The fractal-like outline of the leaf is sculptured by the power of nature, inspiring our bio-fractal structures shown in Figure 1B, in spite of the difference in the incident direction and scale (compared to the optical wavelength) between the real leaf and our plasmonic structures. We discover the Koch curve, one of the earliest fractal geometry described by Helge von Koch in 1904 [1], a good abstraction to mimic the shape of the leaf. The fractal geometry is introduced to the cross section (x–z plane) of the structure and elongated along the y-direction. An ultra-thin layer of gold is deposited on top of the template structure as the active layer for light-matter interactions.

We implement a full-wave finite difference method in time domain method to simulate the optical response of our plasmonic leaf, with results summarised in Figures 2–4. Owing to the translational symmetry along the y-axis, a 2D simulation is applied. The polarisation of the light is along the x, where the electrical field in the x–z plane interacts with the fractal geometry there (TM wave). To investigate the indispensable role played by fractals in light-matter interactions, we model the Koch structures with different fractal orders, as illustrated in Figure 2A. Starting from an equilateral triangle (K1), the structure of the next order can be achieved by removing the inner third of each side, building another equilateral triangle at the location where the side was removed from the previous one. Figure 2B demonstrates the absorption for configurations with different fractal order from 0 to 4. Here, a flat Au film (structure of zeroth-order K0) is used as a reference. In the visible regime where Au is an absorbing material, the absorption enhancement is unambiguously observed as the increment of the fractal order. For the structures with high order (K3, K4), dramatic absorption boost is also achieved in the infrared regime, where only tiny absorption occurs inside the flat thin film (K0, solid red line). We attribute this unconventional effect to the high similarity of the structure at high fractal orders. The same geometry is duplicated at different scales for the fractal structures. Consequently, there is a trend to repeat the spectrum at different wavelength ranges. However, the material dispersion provides a negative impact on the similarity. The competition between the geometric similarity and the optical property dissimilarity produces the spectra as shown in Figure 2C–E. The absorption curves of K4 demonstrate a similar response in different regions through the whole spectrum, generating several absorption peaks in the infrared. As a total effect, a broadband enhancement is observed inside the solar spectrum, as clarified in the inset of Figure 2B, where the enhancement factor is plotted between K4 and K0. The detail for the simulation setup can be found in Supplementary Note 1, and the situation for TE wave (polarisation along the y-axis) can be found in Supplementary Note 2. Simulation results for a different thickness of the Au film are demonstrated in Supplementary Note 3.

Figure 3A summarises the electric field distribution for the structure of different fractal orders with wavelength at 500 nm. Owing to the geometric symmetry, the fields E_x and E_y are shown in the same structure, with the E_x distribution symmetric and the E_y distribution anti-symmetric

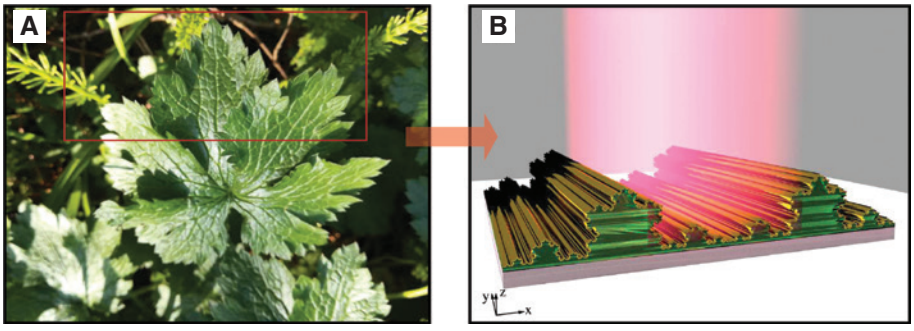

Figure 1: Bio-inspired plasmonic leaf with a fractal structure.
(A) A picture of *Geranium x oxonianum* under the sunshine, harvesting solar energy with optimised light-matter interaction through natural selection. (B) The inspired structure using geometric abstraction from the shape of the leaf. A photoresist template (green) is formed on a glass substrate (grey). A gold film (yellow) is deposited on the template as an energy harvester.

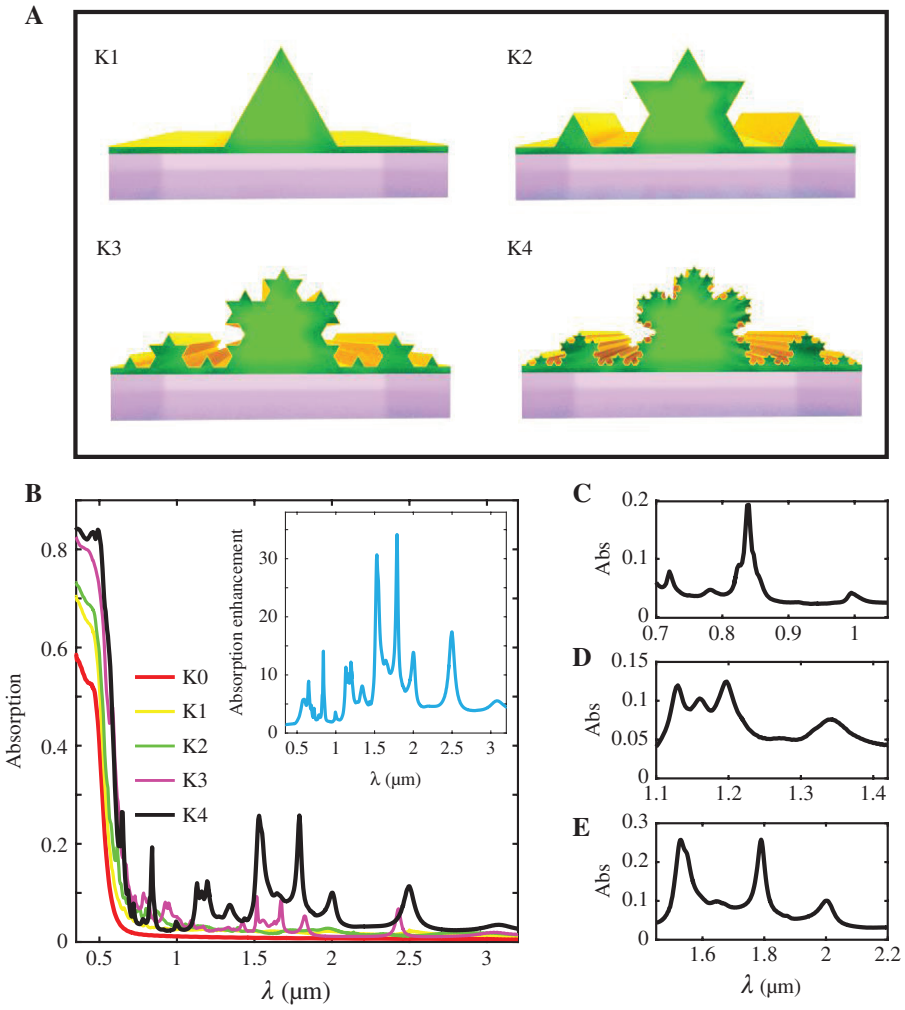

Figure 2: Enhanced absorption of the plasmonic leaf.
(A) Schematic for the structures based on Koch curves with different fractal orders. (B) Absorption spectra of the structures with different fractal orders. The inset shows that the absorption was enhanced between K4 and K0. (C–E) Self-similarity in the absorption from K4. At different wavelength ranges, similar absorption spectra are observed as a result of the fractal geometries.

to $x=0$. For Koch curves, the perimeter is enlarged by a factor of $\frac{4}{3}$ as the fractal order increased by 1, which boosts the light-matter interaction area under the same light power, leading to the absorption improvement shown in Figure 3A. The absorption saturation is not observed at K4, owing to the comparable feature size (180 nm) with optical wavelength. The enhancement factor is not as large as the perimeter enlargement, as a strong interaction (with a large field amplitude) does not occur in all the area. Figure 3B compares the absorption power density:

$$P_{\text{abs}} = -\frac{1}{2}\text{Re}(\nabla \cdot \mathbf{P}), \tag{1}$$

for different structures inside the gold film around $x=0$, demonstrating enhanced absorption ability due to field localisation.

Besides the absorption boost, the intensification of the near field is also a significant benefit from the enhanced light-matter interaction. In Figure 4, we illustrate the intensity enhancement I/I_0 of the K4 structure at different wavelengths, with I_0 the intensity at free space. Owing to the high degree of self-similarity with different feature sizes, the structure is able to achieve strong localisation of photons with different wavelengths in the infrared. Also, sub-wavelength confinement is achieved by virtue of the plasmonic behaviour from gold, as can be seen from Figure 4. Rather interestingly, the fractal geometry assists our plasmonic leaf to tightly confine the light at different wavelengths to the same region, as highlighted by the red/green circles in Figure 4. Such strong localisation of photons with different is always desired for optical systems for energy harvesting and harmonic generations.

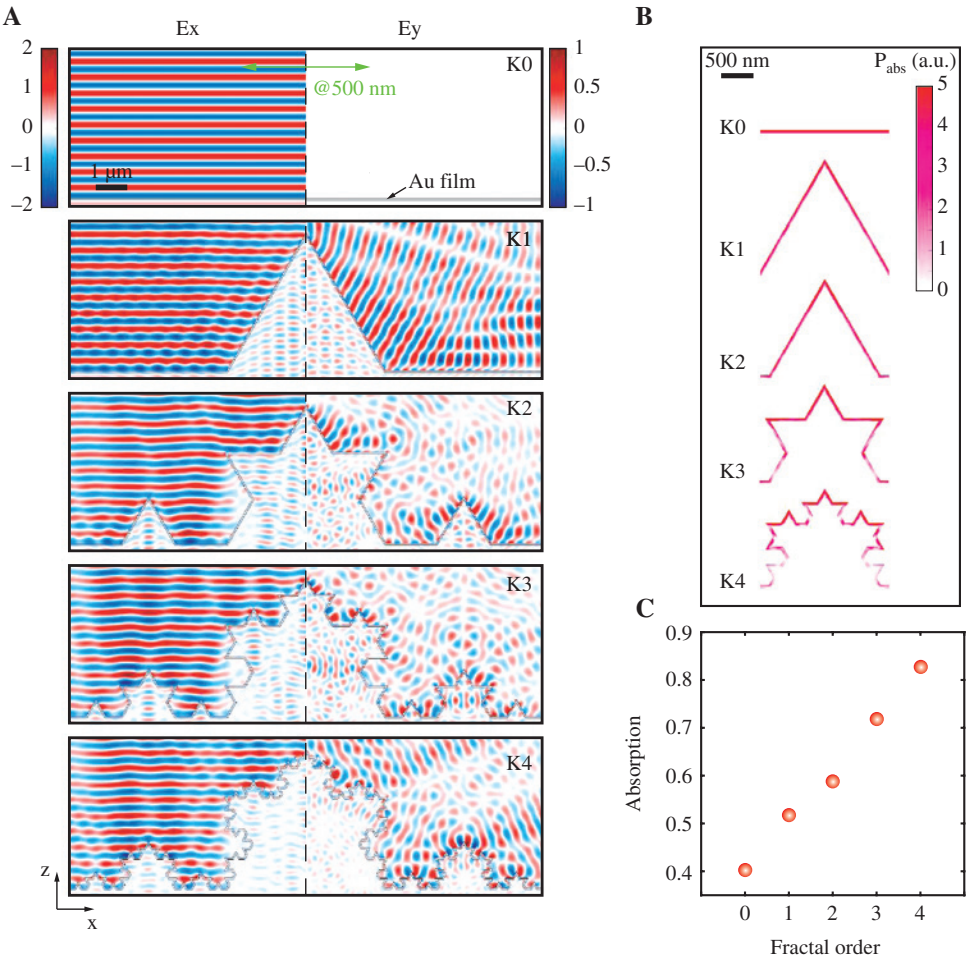

Figure 3: Spatial characterisation of the fractal structures.
(A) Electric field distribution in the x–z plane. E_x is illustrated in the left part and E_y in the right part. Green arrowed line represents the polarisation of the electric field at $\lambda = 500$ nm. (B) The absorption power density P_{abs} of the Au film for structures with fractal order. The region is selected around $x = 0$. (C) The relationship between the absorption and fractal order at $\lambda = 500$ nm.

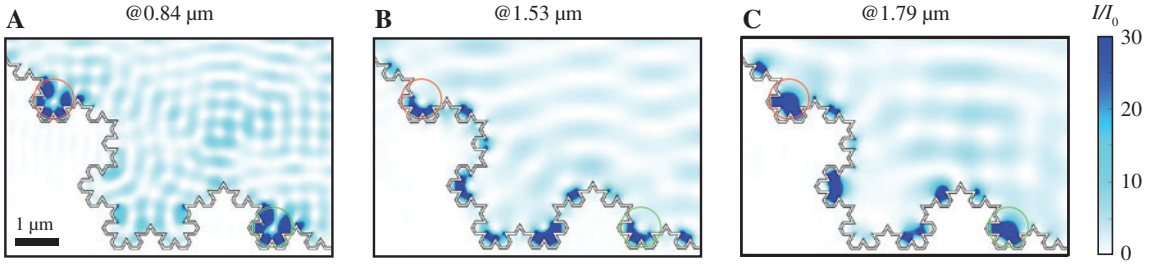

Figure 4: Localising photons with different wavelengths in the same region.
Plasmonic leaf K4 with strong localisation of light for (A) $\lambda = 0.84$ μm, (B) $\lambda = 1.53$ μm, and (C) $\lambda = 1.79$ μm. The light at different wavelengths can be localised to the same region, as marked by the red/green circles.

3 Experimental realisation

The plasmonic leaf is achieved through deposition of Au film on a fractal template made of photoresist through direct laser writing. See Section 5 for more details. Figure 5A–F illustrates the scanning electron microscopy (SEM) images of the fabricated photoresist template through direct laser lithography. Due to the limitation of the resolution, fractal structures are realised up to order of 3. The main geometric features of fractal structures can be realised, with high-resolution features not being precisely copied (such as K3), owing to the fabrication imperfection.

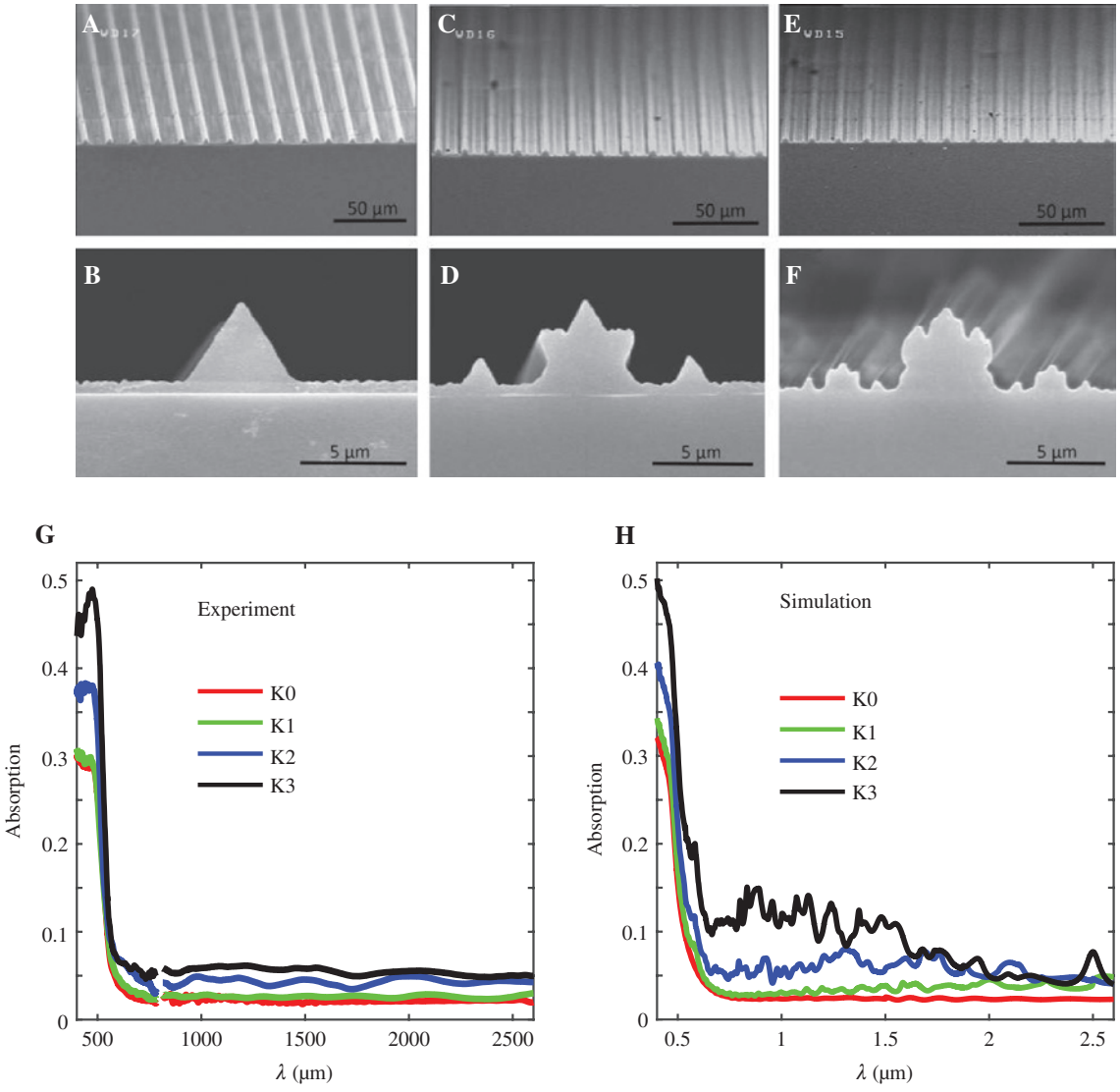

Figure 5: Fabricated samples and absorption characterisation.
(A–C) Titled SEM pictures for fractal structures with different orders: (A) K1, (B) K2, and (C) K3. (D–F) The corresponding zoomed-in cross-section pictures with different orders: (D) K1, (E) K2, and (F) K3. (G, H) The absorption spectra from (G) experiment and (H) simulation.

The absorption of the fractal structures with different orders is investigated, as summarised in Figure 5G. Considering the diffraction/scattering effect, an integrating sphere is used for collecting both the specular and diffusive reflections during the measurement. As the increment of the fractal order, the light-matter interactions are enhanced, leading to the improvement of the absorption. As a result of the self-similarity in fractal structures, a broadband enhancement is observed from 400 to 2400 nm, matching the predictions from the simulation. Instead of a linear polarised light source, an unpolarised beam is used for the absorption measurement, driving the results the averaged value between the TM and TE waves. Correspondingly, Figure 5H illustrates the simulated absorption spectra from the average of both the TE and TM waves. (The separated absorption spectra for TE and TM waves can be found in Supplementary Note 3). The thickness of the Au film is selected to be 10 nm to match the experiment. We attribute the degradation of the experiments to the fabrication imperfection of the fractal template (deformation of the shape, blunting the sharp angles as shown in Figure 5) and the non-uniform coverage of the gold film during the thermal evaporation. Besides, the disorder from the fabrication also broadens the absorption peaks, as predicted from the simulations [23].

To illustrate the enhancement more straightforwardly, we implement the photothermal conversion experiments based on our energy harvester with different fractal orders. Besides photovoltaics that directly

transfer solar energy to electricity, photothermal conversion provides an alternative path to utilise solar energy in versatile ways, including vapour generation and water desalination [24–27], thermophotovoltaics [28–30], and catalysis [31, 32]. Here, a solar simulator is utilised as the light source mimicking the broadband solar radiation. The temperature variation for nanostructures with different fractal orders is summarised in Figure 6. Figure 6A–C represents the spatial temperature distribution for the template only (without Au film), while Figure 6D–F corresponds to the ones with 10-nm-thick gold film as an energy harvester. Without gold film, the template is almost transparent, with negligible temperature increment compared to the room temperature (20°C). Figure 6D–F unambiguously demonstrates the enhanced photothermal conversion as the increase of fractal order from K1 to K3. The active region with fractal geometries is marked with green dashed line, illustrating a prominent temperature increment. Quantitatively, the temperature increment for K1, K2, and K3, are 1.8°C, 4.1°C, and 5.5°C, respectively. The region outside the dashed line is composed on flat Au film with 10 nm thickness, leading to a moderate temperature increment of 0.4°C. The flat Au film itself is a good reflector, especially at the near-infrared region. By virtue of the bio-inspired fractal geometry, we greatly enhance the absorption of such thin film for capturing solar energy as heat, improving the temperature increase by a factor of 14.

4 Discussion

The absorption of the flat Au film decreases drastically from visible to infrared due to its material property, driving Au as a good reflector in the infrared region. Our bio-inspiration utilises the geometric mimic of the outline of Wavegrave Pink, although the underlying mechanism is rather different regarding the light incident directions and the scale compared to the solar wavelength between the real and plasmonic leaves. However, by introducing a plasmonic leaf with fractal structures, not only the enlarged active region but also the geometric self-similarity intensifies the light-matter interactions. Notably, through the competition between the dispersion (making Au reflective) and the high-order self-similarity (reproducing the absorption feature in the visible), strong absorption enhancement is observed both numerically and experimentally. Besides the absorption characterisation, we implement photothermal conversion to directly mapping the improved energy harvesting ability by the temperature increment for an ultra-thin Au film from 0.4°C to 5.5°C. For the feasibility of both simulations and fabrications, the fractal geometry is only introduced to the x–z plane, with no geometric variation along the y-axis. Correspondingly, the absorption in the TE case is reduced compared with TM, as can be found in Supplementary Notes 2 and 3. By virtue of the flexibility of direct laser writing, fractals can be further developed along the y-axis to further enhance

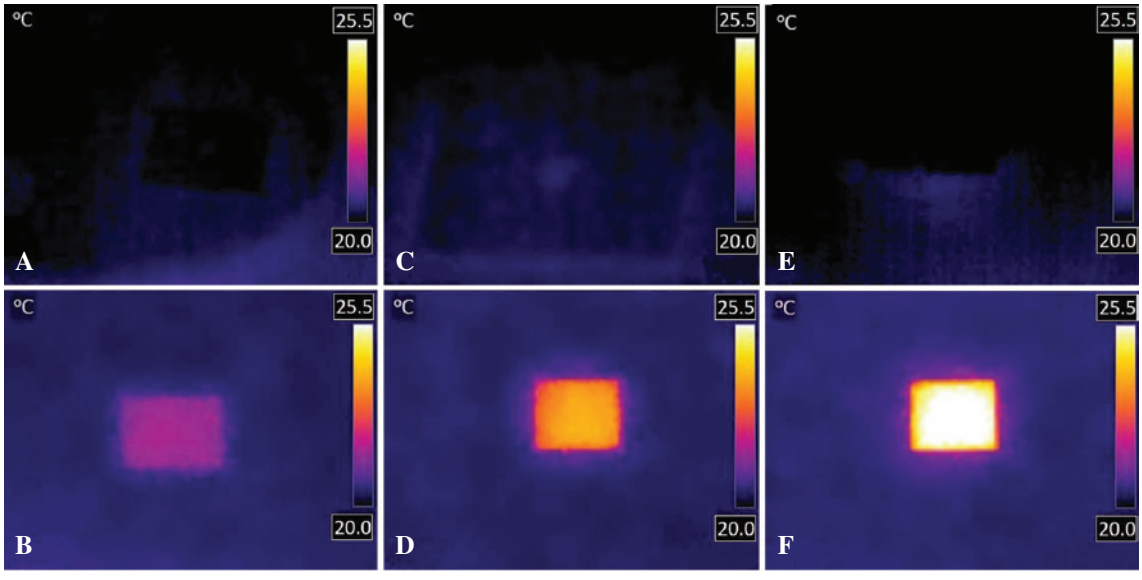

Figure 6: Experiments for photothermal conversion.
(A, C, E) Temperature distribution of the fractal structures K1–K3 without Au film as a reference. (B, D, F) Temperature distribution of the fractal structures K1–K3 with a 10-nm-thick Au film. The active region containing fractal geometry is inside the dashed box. Room temperature is kept at 20°C.

the performance. Besides the photothermal experiments demonstrated here, more sophisticated applications related to energy harvesting, such as photovoltaics [33], could be realised based on the artificial leaf.

The absolute absorption ability and consequently the photothermal conversion efficiency of the fractal structures may not be as good as some other Au-based absorbers [22, 34], especially considering the fabrication complexity. However, self-similarity provides an alternative mechanism other than utilising multiple resonances or geometric singularity (according to transformation optics) to improve the absorption in a broadband way. The complexity caused by the self-similarity strengthens the light-matter interaction at different scales and thus enhances the absorption in a wide spectrum. More importantly, it enables the localisation of multiple wavelengths in the same region (as shown in Figure 3), which is difficult for multi-resonant systems. Besides potential applications in the enhancement of fluorescence [35] and surface-enhanced Raman scattering [36], such spatial field enhancement for multiple wavelengths would be desirable for a plethora of systems based on cooperative effect, such as the second/third harmonic generations [37, 38] and hot electron generations [39]. To further enlarge the light-matter interactions, additional plasmonic nanostructures (such as nanoclusters) can be deposited onto the fractal structure for better performance [40].

5 Methods

5.1 Fabrication and characterisation of the samples

The fractal structures consist of a photopolymer resist (IP-Dip) and were 3D-printed on a glass slide by direct laser lithography [41] (Photonic Professional GT system, Nanoscribe GmbH, Eggenstein, Baden-Württemberg, Germany). The Au film was deposited on the surface of the 3D fractal structures by using a high-vacuum thermal evaporation coating system (Suzhou SinoRaybo Nanotechnology Co., Ltd, Suzhou, Jiangsu, China.

Gold granules (~5 mm) (purchased from Alfa Aesar, Ward Hill, MA, USA) with high purity (99.999%) were used as evaporation source. A direct current power supply was used for heating the tantalum crucible and evaporating the Au granules in high vacuum with a pressure of $1–2\times10^{-4}$ Pa.

The deposition rate was monitored by using a quartz crystal microbalance. During the deposition, the flux can be cut off by a shutter instantly to make a careful control of the deposition thickness. The samples were placed on a substrate holder equipped on the deposition chamber of the system. In this deposition, to avoid a non-uniform deposition of the Au film on the fractal structure surface, the substrate holder keeps rotating clockwise and counterclockwise alternately. The structure of the fractal samples were characterised by SEM (Hitachi S4800Hitachi, Shinagawa, Tokyo, Japan). The evolution of the optical absorption properties of the samples was measured with a spectrophotometer (Zolix Omni-λ300i, Beijing, China).

5.2 Temperature measurement

The surface temperature distribution of test samples was recorded by using an infrared thermal camera (FLIR Merlin MID Infrared Camera, T660 FLIR Systems, Wilsonville, OR, USA). All temperature experiments were conducted using a solar simulator (Newport 94043A, Irvine, CA, USA) accompanied by adjustable optical components (Newport Oriel 67005, Irvine, CA, USA). The solar illumination power was monitored using the Thorlabs PM100D power meter (Thorlabs, Newton, NJ, USA) and controlled at 1 kW/m^2.

Acknowledgements: The work was supported by H2020 European Research Council, Funder Id: http://dx.doi.org/10.13039/100010663, Project Nos. 734578 (D-SPA) and 648783 (TOPOLOGICAL); Leverhulme Trust (grant no. RPG-2012-674); the Royal Society, Wolfson Foundation, National Natural Science Foundation of China (Funder Id: http://dx.doi.org/10.13039/501100001809, grant no. 11604161); the Jiangsu Provincial Natural Science Foundation (grant no. BK20160914); Natural Science Foundation of the Jiangsu Higher Education Institutions of China (grant no. 16KJB140009); Natural Science Foundation of Nanjing University of Posts and Telecommunications (Grant no. NY216012), and the European Union's Horizon 2020 research and innovation programme under the Marie Skłodowska-Curie Grant (grant no. 752102).

Competing interests: The authors declare no conflicts of interest.

References

[1] Mandelbrot BB. The fractal geometry of nature, vol. 173. New York: WH Freeman, 1983.
[2] Miyamaru F, Saito Y, Takeda MW, et al. Terahertz electric response of fractal metamaterial structures. Phys Rev B 2008;77:045124.

[3] Agrawal A, Matsui T, Zhu W, Nahata A, Vardeny Z. Terahertz spectroscopy of plasmonic fractals. Phys Rev Lett 2009;102:113901.
[4] Maraghechi P, Elezzabi A. Enhanced THz radiation emission from plasmonic complementary Sierpinski fractal emitters. Opt Express 2010;18:27336–45.
[5] Kenney M, Grant J, Shah YD, Escorcia-Carranza I, Humphreys M, Cumming DRS. Octave-spanning broadband absorption of terahertz light using metasurface fractal-cross absorbers. ACS Photon 2017;4:2604–12.
[6] De Zuani S, Reindl T, Rommel M, Gompf B, Berrier A, Dressel M. High-order Hilbert curves: fractal structures with isotropic, tailorable optical properties. ACS Photon 2015;2:1719–24.
[7] Bellido EP, Bernasconi GD, Rossouw D, Butet J, Martin OJF, Botton GA. Self-similarity of plasmon edge modes on Koch fractal antennas. ACS Nano 2017;11:11240–9.
[8] Aygar AM, Balci O, Cakmakyapan S, Kocabas C, Caglayan H, Ozbay E. Comparison of back and top gating schemes with tunable graphene fractal metasurfaces. ACS Photon 2016;3:2303–7.
[9] Gottheim S, Zhang H, Govorov AO, Halas NJ. Fractal nanoparticle plasmonics: the Cayley tree. ACS Nano 2015;9:3284–92.
[10] Aslan E, Aslan E, Wang R, et al. Multispectral Cesaro-type fractal plasmonic nanoantennas. ACS Photon 2016;3:2102–11.
[11] Wen W, Zhou L, Li J, Ge W, Chan CT, Sheng P. Subwavelength photonic band gaps from planar fractals. Phys Rev Lett 2002;89:223901.
[12] Navarro-Cia M, Maier SA. Broad-band near-infrared plasmonic nanoantennas for higher harmonic generation. ACS Nano 2012;6:3537–44.
[13] Volpe G, Volpe G, Quidant R. Fractal plasmonics: subdiffraction focusing and broadband spectral response by a Sierpinski nanocarpet. Opt Express 2011;19:3612–8.
[14] Zhu L-H, Shao MR, Peng RW, Fan RH, Huang XR, Wang M. Broadband absorption and efficiency enhancement of an ultrathin silicon solar cell with a plasmonic fractal. Opt Express 2013;21:A313–23.
[15] Abdellatif S, Kirah K. Nanowire photovoltaic efficiency enhancement using plasmonic coupled nano-fractal antennas. Opt Lett 2013;38:3680–3.
[16] Hou C, Meng G, Huang Q, et al. Ag-nanoparticle-decorated Au-fractal patterns on bowl-like-dimple arrays on Al foil as an effective SERS substrate for the rapid detection of PCBs. Chem Commun 2014;50:569–71.
[17] De Nicola F, Purayil NSP, Spirito D, et al. Multiband plasmonic Sierpinski carpet fractal antennas. ACS Photon 2018;5:2418–25.
[18] Fang J, Wang D, DeVault CT, et al. Enhanced graphene photodetector with fractal metasurface. Nano Lett 2016;17:57–62.
[19] Shi NN, Tsai CC, Camino F, Bernard GD, Yu N, Wehner R. Keeping cool: enhanced optical reflection and radiative heat dissipation in Saharan silver ants. Science 2015;349:298–301.
[20] Siddique RH, Donie YJ, Gomard G, et al. Bioinspired phase-separated disordered nanostructures for thin photovoltaic absorbers. Sci Adv 2017;3:e1700232.
[21] Schmager R, Fritz B, Hünig R, et al. Texture of the viola flower for light harvesting in photovoltaics. ACS Photon 2017;4:2687–92.
[22] Huang J, Liu C, Zhu Y, et al. Harnessing structural darkness in the visible and infrared wavelengths for a new source of light. Nat Nanotechnol 2016;11:60–6.
[23] Liu C, Di Falco A, Molinari D, et al. Enhanced energy storage in chaotic optical resonators. Nat Photon 2013;7:473–8.
[24] Zhou L, Tan Y, Wang J, et al. 3D self-assembly of aluminium nanoparticles for plasmon-enhanced solar desalination. Nat Photon 2016;10:393–8.
[25] Liu C, Huang J, Hsiung C-E, et al. High-performance large-scale solar steam generation with nanolayers of reusable biomimetic nanoparticles. Adv Sustain Syst 2017;1:1600013.
[26] Song H, Liu Y, Liu Z, et al. Cold vapor generation beyond the input solar energy limit. Adv Sci 2018:1800222.
[27] Tao P, Ni G, Song C, et al. Solar-driven interfacial evaporation. Nat Energy 2018;3:1031–41.
[28] Lenert A, Bierman DM, Nam Y, et al. A nanophotonic solar thermophotovoltaic device. Nat Nanotechnol 2014;9:126–30.
[29] Fiorino A, Zhu L, Thompson D, et al. Nanogap near-field thermophotovoltaics. Nat Nanotechnol 2018;13:806–11.
[30] Bierman DM, Lenert A, Chan WR, et al. Enhanced photovoltaic energy conversion using thermally based spectral shaping. Nat Energy 2016;1:16068.
[31] Meng X, Wang T, Liu L, et al. Photothermal conversion of CO_2 into CH_4 with H_2 over group VIII nanocatalysts: an alternative approach for solar fuel production. Angew Chem Int Ed 2014;53:11478–82.
[32] Sarina S, Zhu H-Y, Xiao Q, et al. Viable photocatalysts under solar-spectrum irradiation: nonplasmonic metal nanoparticles. Angew Chem Int Ed 2014;53:2935–40.
[33] Labelle A, Bonifazi M, Tian Y, et al. Broadband epsilon-near-zero reflectors enhance the quantum efficiency of thin solar cells at visible and infrared wavelengths. ACS Appl Mater Interfaces 2017;9:5556–65.
[34] Søndergaard T, Novikov SM, Holmgaard T, et al. Plasmonic black gold by adiabatic nanofocusing and absorption of light in ultra-sharp convex grooves. Nat Commun 2012;3:969.
[35] Dong J, Zhang Z, Zheng H, Sun M. Recent progress on plasmon-enhanced fluorescence. Nanophotonics 2015;4:472–90.
[36] Ding S-Y, Yi J, Li J-F, et al. Nanostructure-based plasmon-enhanced Raman spectroscopy for surface analysis of materials. Nat Rev Mater 2016;1:16021.
[37] O'Brien K, Suchowski H, Rho J, et al. Predicting nonlinear properties of metamaterials from the linear response. Nat Mater 2015;14:379–83.
[38] Li G, Zhang S, Zentgraf T. Nonlinear photonic metasurfaces. Nat Rev Mater 2017;2:17010.
[39] Brongersma ML, Halas NJ, Nordlander P. Plasmon-induced hot carrier science and technology. Nat Nanotechnol 2015;10:25–34.
[40] Mao P, Liu C, Favraud G, et al. Broadband single molecule SERS detection designed by warped optical spaces. Nat Commun 2018;9:5428.
[41] Thiel M, Hermatschweiler M. Three-dimensional laser lithography: a new degree of freedom for science and industry. Opt Photon 2011;6:36–9.

Supplementary Material: The online version of this article offers supplementary material (https://doi.org/10.1515/nanoph-2019-0104).